Generalized Bessel functions in tunnelling ionization

2003 J. Phys. A: Math. Gen. 36 5575

(http://iopscience.iop.org/0305-4470/36/20/313)

INSTITUTE OF PHYSICS PUBLISHING JOURNAL OF PHYSICS A: MATHEMATICAL AND GENERAL

J. Phys. A: Math. Gen. **36** (2003) 5575–5585 PII: S0305-4470(03)59704-9

Generalized Bessel functions in tunnelling ionization

H R Reiss[1,2] **and V P Krainov**[3]

[1] Departamento de Fisica Aplicada, Universidad de Salamanca, 37008 Salamanca, Spain
[2] Physics Department, American University, Washington, DC 20016-8058, USA
[3] Moscow Institute of Physics and Technology, 141700 Dolgoprudny, Moscow Region, Russia

Received 17 February 2003, in final form 31 March 2003
Published 7 May 2003
Online at stacks.iop.org/JPhysA/36/5575

Abstract
We develop two new approximations for the generalized Bessel function that frequently arises in the analytical treatment of strong-field processes, especially in non-perturbative multiphoton ionization theories. Both these new forms are applicable to the tunnelling environment in atomic ionization, and are analytically much simpler than the currently used low-frequency asymptotic approximation for the generalized Bessel function. The second of the new forms is an approximation to the first, and it is the second new form that exhibits the well-known tunnelling exponential.

PACS numbers: 02.30.Gp, 02.60.Gf, 32.80.Rm, 42.50.Hz

1. Introduction

The generalized Bessel function appears in problems involving physical systems subjected to intense plane-wave electromagnetic fields. It occurs when the Volkov [1] (or Gordon [2]–Volkov) solution is employed in an analytical approximation. Applications can be as diverse as relativistic elementary particle problems, where the generalized Bessel function was first encountered and defined [3]; or problems in strong-field atomic ionization, where it is currently widely employed. An extensive listing of the properties of the generalized Bessel function can be found in the appendices of [4], and in appendix J of [5].

Currently, the most common type of problem in which the generalized Bessel function appears is in application of the SFA [4] (strong-field approximation) to laser–atom interaction physics with linearly polarized laser fields. This application most often relates to the tunnelling regime, since the field intensity may be quite high, but the energy of a single photon of the laser is generally much less than the ionization potential of the atom. The tunnelling environment involves a combination of high-order processes and strong fields. We seek here to develop an approximation specifically for the tunnelling regime that is much simpler than the algebraically cumbersome asymptotic form developed in appendix D of [4]. That earlier result, referred to hereafter as the 'asymptotic approximation', is reproduced in the appendix at the end of this paper.

The generalized Bessel function is defined either by the integral form

$$J_n(u, v) = \frac{1}{2\pi} \int_{-\pi}^{\pi} d\varphi \exp[i(u \sin\varphi + v \sin 2\varphi - n\varphi)] \tag{1}$$

or by the equivalent series representation

$$J_n(u, v) = \sum_{k=-\infty}^{\infty} J_{n-2k}(u) J_k(v). \tag{2}$$

Here $J_k(v)$ is the usual Bessel function. We consider only integer values of the order n, and real values of the arguments u, v.

For the current laboratory environment of strong-field multiphoton atomic ionization by low-frequency fields, the generalized Bessel function can be extremely difficult to compute in its completely stated form. A low-frequency approximation is eminently useful. The asymptotic approximation is found from a saddle-point analysis of the integral form (equation (1)). The purpose of the present work is to give an alternative form found from a physically motivated approach. The tunnelling approximation we find has a straightforward analytical expression, but it is not quite in the familiar tunnelling form since it does not transparently exhibit the characteristic tunnelling exponential $\exp(-C/F)$, where C depends on the parameters of the problem, and F is the magnitude of the electric field. At a second level of approximation, we do indeed find the familiar tunnelling exponential.

2. Tunnelling conditions

In multiphoton ionization, the electromagnetic field must supply both the zero-field binding energy of the atom, given by the positive quantity E_B, and the ponderomotive energy U_p required for the ionized electron to possess at least the oscillation energy of a free electron in the field. The threshold photon order is the smallest integer n_0 such that

$$n_0\omega \geqslant E_B + U_p \tag{3}$$

where ω is the frequency of the laser field, and atomic units are used. By hypothesis, the field is of low frequency, and so the photon order, $n \geqslant n_0$, must be large:

$$\omega \ll E_B \qquad n \gg 1. \tag{4}$$

To achieve ionization at a large multiphoton order, the field must be intense in the sense that

$$z \equiv U_p/\omega \gg 1. \tag{5}$$

The tunnelling conditions, equations (3)–(5), are sufficient to place constraints on the parameters n, u, v that define the generalized Bessel function $J_n(u, v)$. As they occur in the SFA, we have

$$u = (z/\omega)^{1/2} 2p \cos\theta \tag{6}$$

$$v = -z/2. \tag{7}$$

The properties of the v variable are completely straightforward from equations (5) and (7):

$$v < 0 \qquad |v| \gg 1. \tag{8}$$

The momentum p within the SFA is, from energy conservation conditions,

$$p = \sqrt{2\omega(n - z - \epsilon_B)} = \sqrt{2\omega(n - n_0)} \tag{9}$$

$$\epsilon_B \equiv E_B/\omega. \tag{10}$$

We can take $\cos\theta = 1$ in equation (6). Tunnelling occurs with low velocity of the ionized electron, so $n \approx n_0$. If we take $n - n_0 \leqslant 10$, then $p \leqslant \sqrt{20\omega}$. This gives $u \leqslant 2\sqrt{20z}$. The result is that u can be quite large, since z is large. On the other hand, we have to consider that it is possible to have $p = 0$, or to have $\cos\theta = 0$, so that

$$0 \leqslant u_{\min} \qquad u_{\max} \gg 1. \tag{11}$$

To find more definitive constraints on u, we can compare it with v. We have a limit on u that depends only on z, so we can compare u directly with $|v|$, giving the result

$$\frac{u}{|v|} \leqslant \frac{2\sqrt{20z}}{z/2} \approx \frac{20}{z^{1/2}} \ll 1. \tag{12}$$

To summarize, the n, u, v parameters of $J_n(u, v)$ in the tunnelling regime are subject to the limits

$$n \gg 1 \qquad |v| \gg 1, \quad v < 0 \qquad 0 \leqslant u \ll |v|. \tag{13}$$

3. Tunnelling approximation for $J_n(u, v)$

The above results make it possible to start with the integral representation of equation (1), and do a steepest-descent approximation with the saddle-point locations determined by the n and v parameters in the exponent. The part of the exponent dependent on u can then be evaluated at the saddle points determined by n and u. The integral representation in equation (1) can thus be written as

$$J_n(u, v) = \frac{1}{2\pi}\int_{-\infty}^{\infty} \mathrm{d}\theta \exp(\mathrm{i}u\sin\theta)\,\mathrm{e}^{zg(\theta)} \tag{14}$$

$$g(\theta) = \mathrm{i}\left(\frac{v}{z}\sin 2\theta - \frac{n}{z}\theta\right) \tag{15}$$

where z is the large parameter needed for the steepest-descent approximation, and the saddle points are determined by $\mathrm{d}g/\mathrm{d}\theta = 0$. When we insert $v = -z/2$ and define $\alpha \equiv n/z$, then

$$g(\theta) = -\mathrm{i}\left(\tfrac{1}{2}\sin 2\theta + \alpha\theta\right) \tag{16}$$

and the saddle-point locations θ_0 are where $g'(\theta) = -\mathrm{i}(\cos 2\theta + \alpha) = 0$, or

$$\cos 2\theta_0 = -\alpha. \tag{17}$$

We know from equation (3) that $n > z$, so $\alpha > 1$ and the saddle points must be off the real axis. If we set $\theta_0 = x + \mathrm{i}y$, then

$$\sin 2x \sinh 2y = 0 \tag{18}$$

$$\cos 2x \cosh 2y = -\alpha. \tag{19}$$

Equation (18) gives $\sin 2x = 0$ since $y \neq 0$. Equation (19) requires that $\cos 2x < 0$, so we know the saddle points must be at

$$x = \pm\frac{\pi}{2} \qquad y = \frac{1}{2}\cosh^{-1}\alpha. \tag{20}$$

This gives four saddle points, but we know that at those saddle points through which we can pass a path of steepest descent, we must have $g''(\theta) < 0$. We have

$$g''(\theta_0) = \mathrm{i}2\sin 2\theta_0 \tag{21}$$

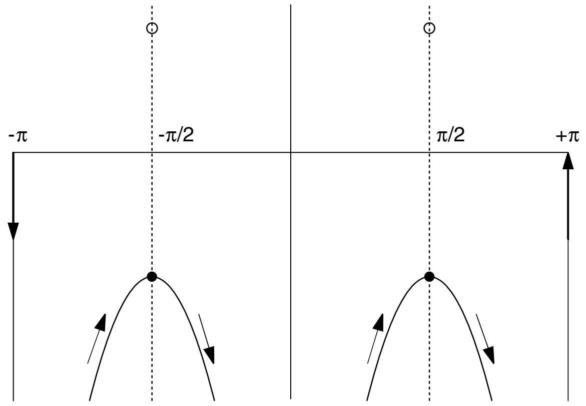

Figure 1. The deformed path of integration in the complex θ plane needed to evaluate $J_n(u, v)$ by the method of steepest descent is shown by the arrows. With θ separated into real and imaginary parts in terms of $\theta = \theta_r + \mathrm{i}\theta_i$ (θ_r, θ_i real), the amplitude of $\exp[g(\theta)]$, as defined in equations (14) and (15), goes to zero exponentially in the lower half-plane ($\theta_i < 0$) in the intervals $-\pi < \theta_r < -3\pi/4$, $-\pi/4 < \theta_r < \pi/4$ and $3\pi/4 < \theta_r < \pi$. This explains the shape of the path shown between the original end points of the integral at $(-\pi, \pi)$, and the path deformed to pass through the saddle points in the lower half-plane shown by the solid circles.

$$\sin 2\theta_0 = \sin 2x \cosh 2y + \mathrm{i}\cos 2x \sinh 2y = -\mathrm{i}\sinh 2y \tag{22}$$

$$g''(\theta_0) = 2\sinh 2y. \tag{23}$$

Since $g''(\theta) < 0$ along the deformed path we follow, this means that the necessary saddle points are the two that are in the lower half of the complex plane at

$$x = \pm\frac{\pi}{2} \qquad y = -\frac{1}{2}|\cosh^{-1}\alpha|. \tag{24}$$

Figure 1 shows how the original real-axis path of integration is deformed in the complex θ plane to pass through the two saddle points in the lower half-plane, such that only that part of the path near the saddle points contributes to the result. This gives

$$\sinh 2y = -\sqrt{\alpha^2 - 1} \tag{25}$$

$$g''(\theta_0) = -2\sqrt{\alpha^2 - 1} \tag{26}$$

$$g(\theta_0) = -\mathrm{i}\left(\frac{1}{2}\sin 2\theta_0 + \alpha\theta_0\right) = -\mathrm{i}\left(-\frac{\mathrm{i}}{2}\sinh 2y \pm \frac{\pi}{2}\alpha - \mathrm{i}\frac{\alpha}{2}|\cosh^{-1}\alpha|\right) \tag{27}$$

$$= \frac{1}{2}\sqrt{\alpha^2 - 1} - \frac{\alpha}{2}|\cosh^{-1}\alpha| \mp \mathrm{i}\frac{\pi}{2}\alpha. \tag{28}$$

We must also consider the multiplier $\exp(\mathrm{i}u\sin\theta_0)$:

$$\sin\theta_0 = \sin x \cosh\left(-\frac{1}{2}|\cosh^{-1}\alpha|\right) \tag{29}$$

$$= \pm\sqrt{\frac{1}{2}(1 + \cosh(\cosh^{-1}\alpha))} \tag{30}$$

$$= \pm\sqrt{\frac{1+\alpha}{2}} \tag{31}$$

$$\exp(\mathrm{i}u\sin\theta_0) = \exp(\pm\mathrm{i}u\sqrt{(1+\alpha)/2}). \tag{32}$$

We can now write the result for $J_n(u, v)$:

$$J_n(u,v) = \frac{\exp\left(\frac{z}{2}\sqrt{\alpha^2-1} - \frac{z\alpha}{2}|\cosh^{-1}\alpha|\right)}{\sqrt{4\pi z\sqrt{\alpha^2-1}}}\Big[\exp\left(\mathrm{i}u\sqrt{(1+\alpha)/2} - \mathrm{i}\pi z\alpha/2\right) + \exp\left(-\mathrm{i}u\sqrt{(1+\alpha)/2} + \mathrm{i}\pi z\alpha/2\right)\Big]. \tag{33}$$

This can be simplified using $z\alpha = n$ and combining the last square bracket into a cosine function, to get

$$J_n(u,v) = \frac{\exp\left(\frac{1}{2}\sqrt{n^2-z^2} - \frac{n}{2}\left|\cosh^{-1}\frac{n}{z}\right|\right)}{\sqrt{\pi}(n^2-z^2)^{1/4}}\cos\left(u\sqrt{\frac{n+z}{2z}} - \frac{n\pi}{2}\right). \tag{34}$$

Equation (34) is the primary result of this paper. This form will be referred to as 'tunnelling 1', since a second tunnelling approximation will be developed below.

Note the very simple dependence in equation (34) on the u parameter. However, equation (34) also shows that if n is varied with z held constant, or vice versa, the cosine function does not have simple periodicity. It is also easy to show that the maximum value of the argument of the exponential is zero, achieved when $z = n$. For all smaller values of z, the argument of the exponential is negative. Since, in physical application, $z < n$ always, this means that the exponential always provides damping.

4. Second tunnelling approximation

Although equation (34) has an explicit analytical form far simpler and more transparent than the asymptotic approximation in the appendix, it does not display the characteristic tunnelling exponential $\exp(-C/F)$, where F is the amplitude of the electric field. This result has been known [6] since the early days of quantum mechanics. We shall now do a further approximation that leads to the familiar form.

We work with the parameter α, defined earlier as

$$\alpha \equiv n/z \tag{35}$$

and then set $\alpha = 1 + \eta$. The quantity η is small in the tunnelling domain, since we can rewrite α as

$$\begin{aligned}\alpha &= \frac{n}{z} = 1 + \eta = \frac{(n-n_0) + z + \epsilon_B}{z} \\ &= 1 + \frac{n-n_0}{z} + \frac{\epsilon_B}{z}.\end{aligned} \tag{36}$$

The quantity $(n - n_0)/z$ is small by the tunnelling hypothesis that the ionized electron emerges with very low kinetic energy. The last term in equation (36) can be written as

$$\frac{\epsilon_B}{z} = \frac{E_B/\omega}{U_p/\omega} = \frac{E_B}{U_p} \ll 1. \tag{37}$$

The inequality (37) is a separate strong-field approximation that appeared in [4] as the intensity parameter $z_1 \equiv 2U_p/E_B$. When $z_1 \gg 1$, the effect of the laser field on the ionized electron is much greater than the effect of the Coulomb binding potential. This quantity appeared even earlier as the Keldysh parameter [7]

$$\kappa \equiv \sqrt{E_B/2U_p} = 1\big/z_1^{1/2}. \tag{38}$$

Keldysh showed that this parameter must be small for tunnelling to occur. The last two terms in equation (36) are both small in a tunnelling situation, which means that we can regard the parameter η as a small parameter.

To express the argument of the exponential function in equation (34) in terms of η, we have

$$\frac{1}{2}\sqrt{n^2-z^2}-\frac{n}{2}\left|\cosh^{-1}\frac{n}{z}\right| = \frac{n}{2}\left[\left(\frac{1}{1+\eta}\right)\sqrt{\eta(2+\eta)}-\cosh^{-1}(1+\eta)\right]. \tag{39}$$

Expansion in powers of η gives

$$\left(\frac{1}{1+\eta}\right)\sqrt{\eta(2+\eta)} \approx \sqrt{2\eta}\left(1-\frac{3}{4}\eta+\cdots\right) \tag{40}$$

$$\cosh^{-1}(1+\eta) \approx \sqrt{2\eta}\left(1-\frac{1}{12}\eta+\cdots\right) \tag{41}$$

for a final result

$$\exp\left(\frac{1}{2}\sqrt{n^2-z^2}-\frac{n}{2}\left|\cosh^{-1}\frac{n}{z}\right|\right) \approx \exp\left(-\frac{n}{3}\sqrt{2\eta^3}\right). \tag{42}$$

The denominator in equation (34) reduces to

$$\sqrt{\pi}(n^2-z^2)^{1/4} = \sqrt{\pi n}\left(1-\frac{1}{\alpha^2}\right)^{1/4} = \sqrt{\pi n}\left[\frac{\eta(2+\eta)}{(1+\eta)^2}\right]^{1/4}$$
$$\approx \sqrt{\pi n}(2\eta)^{1/4}\left(1-\frac{3}{8}\eta^{1/2}+\cdots\right) \approx \sqrt{\pi n\sqrt{2\eta}}. \tag{43}$$

Within the argument of the cosine function in equation (34), we can make the reduction

$$\sqrt{\frac{n+z}{2z}} = \sqrt{\frac{2+\eta}{2}} \approx 1+\frac{1}{4}\eta. \tag{44}$$

When the approximations in equations (40)–(44) are incorporated into equation (34), the result is

$$J_n(u,v) \approx \frac{1}{\sqrt{\pi n}(2\eta)^{1/4}}\exp\left(-\frac{n}{3}\sqrt{2\eta^3}\right)\cos\left[u\left(1+\frac{1}{4}\eta\right)-\frac{n\pi}{2}\right]. \tag{45}$$

Within the cosine function, it is necessary to retain the first correction in η. Despite the fact that we have taken $u \ll |v|$ in equation (13), u can nevertheless be large, and the product $u\eta$ makes an important contribution to the phase of the trigonometric function. We also see that the term $n\pi/2$ in the argument of the cosine generally leads to substantial differences between consecutive orders n, even when other parameters remain fixed. Some simplification of equation (45) can be obtained by the substitution

$$\gamma^2 \equiv \tfrac{1}{2}\eta \tag{46}$$

leading to the alternative form

$$J_n(u,v) \approx \frac{1}{\sqrt{2\pi n\gamma}}\exp\left(-\frac{4n\gamma^3}{3}\right)\cos\left[u\left(1+\frac{1}{2}\gamma^2\right)-\frac{n\pi}{2}\right]. \tag{47}$$

Equation (45) or (47) is somewhat simpler than equation (34), although an additional approximation had to be introduced. This new form will be referred to as 'tunnelling 2' to distinguish it from 'tunnelling 1' of equation (34). We can see in equation (47), a hint of the famous tunnelling exponential first found by Oppenheimer [6] for time-independent electric fields. However, equation (47) retains a reference to photon order n, and that is certainly not a feature of tunnelling behaviour.

5. Tunnelling exponential

As remarked above, equations (45) and (47) contain the photon order parameter n, a concept alien to tunnelling theories. The photon order also appears in the trigonometric function, meaning that positive and negative values of $J_n(u, v)$ are about equally likely. This in itself is not a drawback, since transition rates will always involve $[J_n(u, v)]^2$, so the alternation of sign is not critical in exhibiting tunnelling behaviour. The essential behaviour is in the exponential.

Equations (36) and (46) give the connection

$$\gamma = \sqrt{\frac{n-z}{2z}}. \tag{48}$$

In a tunnelling problem, we can set

$$n \approx n_0 = z + \epsilon_B \approx z. \tag{49}$$

This approximation of simply substituting z for n suffices for all appearances of n in equation (47) except in the combination $n - z$ that appears in equation (48). There we must use the more accurate form $n - z = \epsilon_B$. With these replacements, the argument of the exponential in equation (47) is

$$\frac{4n\gamma^3}{3} \approx \frac{1}{3}\sqrt{\frac{2\epsilon_B^3}{3}}. \tag{50}$$

As a final step, we need to double equation (50) to give the exponential associated with $[J_n(u, v)]^2$ when speaking of transition rates rather than transition amplitudes; and we also introduce the definitions of z and ϵ_B from equations (5) and (10). That is, we substitute $z = U_p/\omega = F^2/4\omega^3$ and $\epsilon_B \equiv E_B/\omega$. This gives the final result for the exponential appearing in the tunnelling rate as

$$\exp\left(-\frac{8n\gamma^3}{3}\right) \approx \exp\left[-\frac{2}{3}\frac{(2E_B)^{3/2}}{F}\right]. \tag{51}$$

This has the requisite $\exp(-C/F)$ tunnelling form. It is identical to the tunnelling exponential in equation (81) of [4].

6. Evaluation of the results

To have an overview of the general nature of the generalized Bessel function, figure 2 gives examples for $n = 20$ in part (*a*), and $n = 40$ in part (*b*). The tunnelling regime is in the left foreground of these figures, where $|v| \lessapprox n/2$, and where $u \ll |v|$. A comparison of figure 2(*a*) with 2(*b*) shows how $J_n(u, v)$ changes with increasing order. The oscillations along the line $|v| = n/2$ increase in number, but decrease in their extension into the domain where $|v|$ is less than $n/2$. Also, the 'null' region where $J_n(u, v)$ is approximately zero becomes increasingly extensive with increasing order n. Even more complex features emerge at yet higher orders.

We now show how the tunnelling approximation compares with exact results. Three-dimensional figures become very difficult to decipher, so results are presented for a fixed value of the order n, as in figure 2, but also with a fixed intensity z, corresponding to a fixed value of v. In turn, a value of $|v|$ slightly less than $n/2$ is employed to place the results in the 'active' tunnelling region seen in figure 2.

Figure 3 shows how the tunnelling approximation of equation (34) (tunnelling 1) compares with an exact evaluation of $J_n(u, v)$ when $n = 20$ and v has the fixed value $v = -9$, close to the maximum $|v| = 10$. Although nominally the tunnelling approximation should be confined to $u \ll |v|$, it is seen that the tunnelling approximation gives a reasonable prediction for the

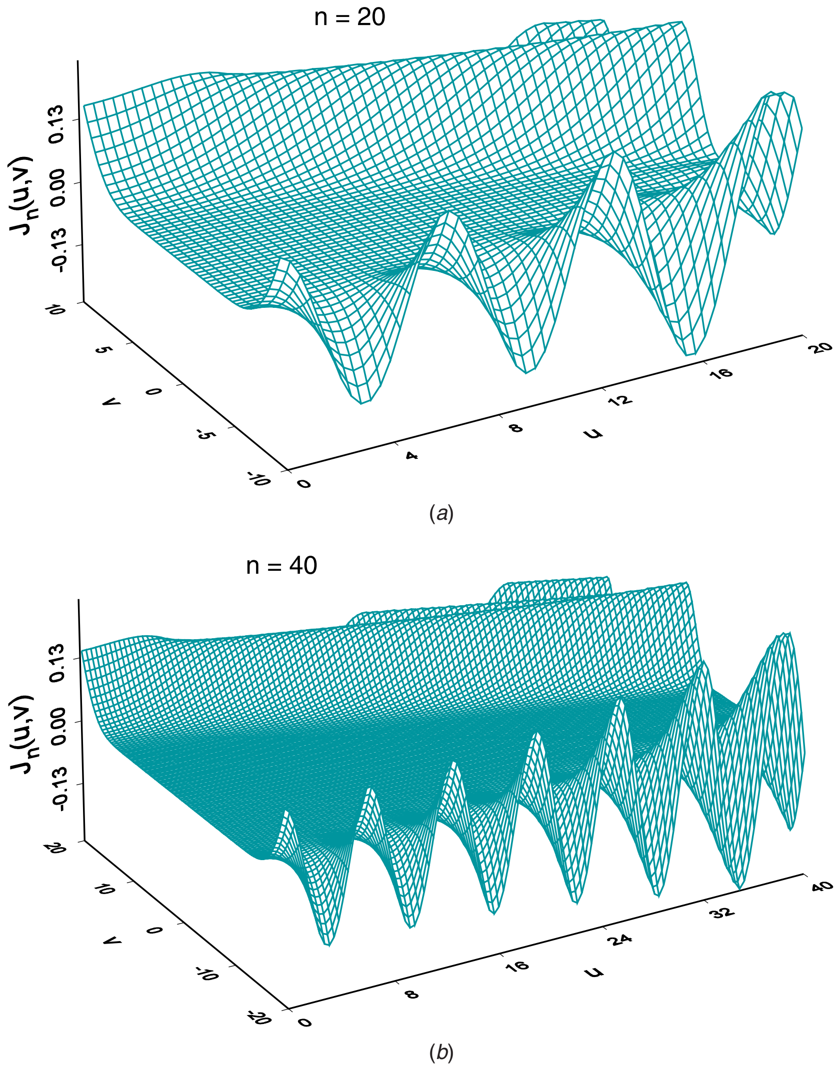

Figure 2. Behaviour of $J_n(u, v)$ as a function of u and v for a fixed order n. Figure 2(a) is for $n = 20$ and figure 2(b) is for $n = 40$. These figures illustrate the general properties that the amplitude of $J_n(u, v)$ is most significant in the region $v \lesssim -n/2$ corresponding to $z \lesssim n$; that $J_n(u, v)$ exhibits almost-periodic oscillations in this region with variable amplitude; and that there is a large domain with $|J_n(u, v)| \ll 1$ (the 'null domain') that increases in extent as n increases. Despite the increasing size of the null domain, the amplitude of the oscillations in $J_n(u, v)$ decreases only very slowly as n increases.

amplitude of the oscillations up to $u = n/4 \approx |v|/2$, and an almost perfect reproduction of the phase and frequency of the oscillation. For this relatively small n value, the tunnelling approximation gives more accurate results than the asymptotic approximation, also shown in figure 3.

Proceeding to the larger value $n = 40$ (and $|v| = 18$) in figure 4, it is seen that the approximation of equation (34) (tunnelling 1) again performs well in all respects up to about $u = n/4$. This corresponds to the limitations expressed in equation (13).

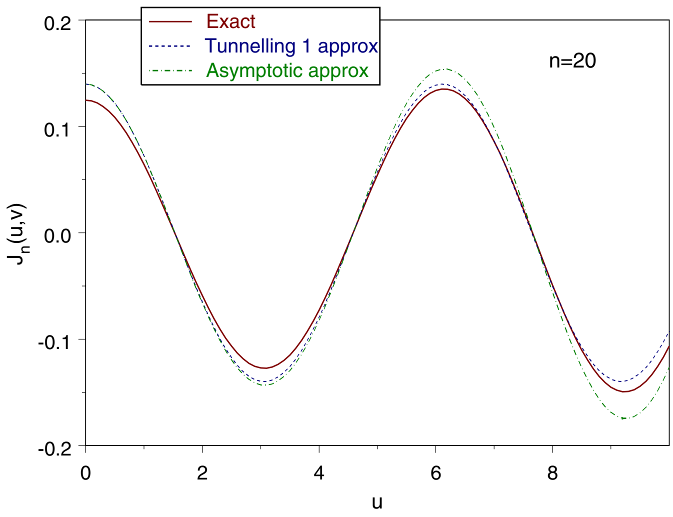

Figure 3. A comparison of the tunnelling approximation for $J_n(u, v)$ of equation (34), shown by the dashed line, the asymptotic approximation (appendix) shown by the dot-dash line, and the exact $J_n(u, v)$ value shown by the full line. Here, $n = 20$, and $|v| = 9$, corresponding to $|v| \lesssim n/2$. The range of u is the interval $0 \leqslant u \leqslant n/2$. In principle, the tunnelling approximation is valid only for the domain where $u \ll |v|$. It is seen that the tunnelling approximation retains its validity over the larger-than-expected range of $0 \leqslant u \leqslant |v|/2$ or $0 \leqslant u \leqslant n/4$.

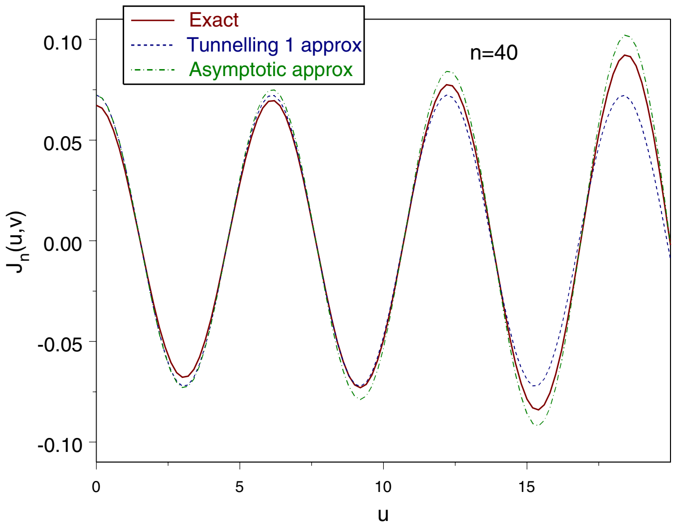

Figure 4. This is similar to figure 3, except that here $n = 40$ and $|v| = 18 \lesssim n/2$. The agreement of the tunnelling 1 approximation (equation (34)) with the exact result is excellent for the range $0 \leqslant u \leqslant n/4$, which exceeds the expected range with $u \ll |v|$. Tunnelling and asymptotic approximations are almost identical for small u, but differ in amplitude for larger u values. Both approximations remain excellent in reproducing accurately the period and phasing of the oscillations.

Figure 5 shows results for $n = 100$ and $|v| = 45$. At this large value of n, the asymptotic approximation is virtually identical to the exact result, so that one curve is shown, with a single

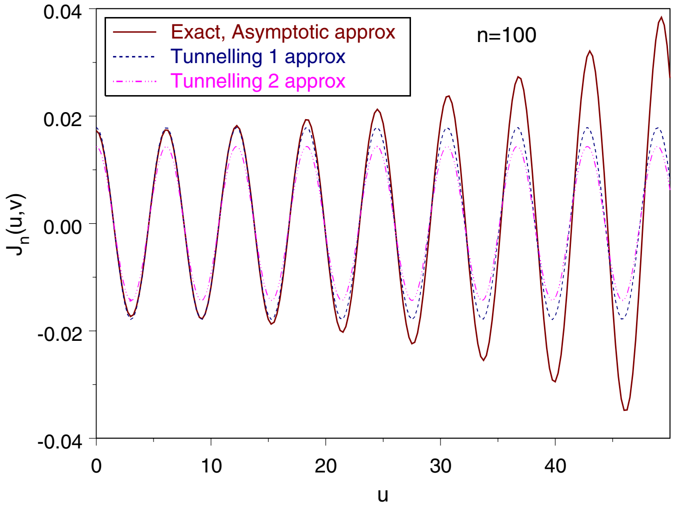

Figure 5. The relatively large value $n = 100$ is shown here. The asymptotic approximation is almost identical to the exact result for this high order, as the legend entry indicates. Reproduction of exact results by tunnelling 1 is again good up to about $u = n/4$, but now there is a clear failure to reproduce amplitude, period, or phase for larger values of u that are plainly outside the tunnelling domain. The second tunnelling approximation, tunnelling 2 (equation (47)), is also shown here. Performance in matching the exact result is satisfactory for tunnelling 2, but not at the level of tunnelling 1.

legend entry identifying it with both the exact and asymptotic forms. This gives an opportunity to compare the two tunnelling forms of equations (34) and (47) without making the figure excessively crowded. Agreement of tunnelling 1 with the exact value is, as in the other cases, very good to $u = n/4$, and essentially perfect for $u < n/8$. Equation (47) (tunnelling 2) is satisfactory, but not as accurate as tunnelling 1, as could be anticipated from the derivations.

Acknowledgments

One author (HRR) extends his thanks to the Spanish Ministerio de Ciencia y Tecnologia for partial support of this work (FEDER funds, grant no BFM2002-00033). The other author (VPK) wishes to thank the Russian Foundation for Basic Research for partial support of this work (projects N 01-02-16056 and 02-02-16678).

Appendix

The tunnelling approximation to $J_n(u, v)$ given in equation (34) is a relatively simple algebraic expression that computes very rapidly in a computational application. The asymptotic form found in [4] is also a direct algebraic result, free of integrations, summations or any mathematical form requiring iterations. Nevertheless, the form found here is so very much simpler than that of [4], that is has been found to compute 5 to 10 times faster in practical applications than the earlier result. For completeness, the earlier result is reproduced below, with the explicit replacement of the parameter v by the quantity $-z/2$, as employed above in equation (7). This earlier result was found by a procedure similar to the one used here, except that the saddle-point locations were determined from the combined influence of all of the n, u, v parameters, rather than just n and v, as done in equation (14). The asymptotic form for $J_n(u, v)$ found in [4] is

$$J_n\left(u, -\frac{z}{2}\right) \approx \frac{(2z^{1/2})^n}{(2\pi QR)^{1/2}} \frac{[(Q^{1/2}+U^{1/2})^{1/2}\cos\chi - (Q^{1/2}-U^{1/2})^{1/2}\sin\chi]}{[(n+z+Q)^{1/2}+(n-3z+Q)^{1/2}]^n} \times \exp\left[\frac{RU^{1/2}}{2} + \frac{3u(Q-U)^{1/2}}{4(2z)^{1/2}}\right]$$

$$\chi \equiv \frac{3uU^{1/2}}{4(2z)^{1/2}} - \frac{R(Q-U)^{1/2}}{2} - n\arccos\left[\frac{(n+z-Q)^{1/2}}{2z^{1/2}}\right]$$

$$Q \equiv [(n+z)^2 - u^2]^{1/2}$$

$$R \equiv \left(n - z - \frac{u^2}{8z}\right)^{1/2}$$

$$U \equiv \frac{1}{2}(n+z+Q) - \frac{u^2}{8z}.$$

References

[1] Volkov D M 1935 *Z. Phys.* **94** 250

[2] Gordon W 1926 *Z. Phys.* **40** 117

[3] Reiss H R 1962 *J. Math. Phys.* **3** 59 appendix B

[4] Reiss H R 1980 *Phys. Rev.* A **22** 1786 appendices B–D

[5] Krainov V P, Reiss H R and Smirnov B M 1997 *Radiative Processes in Atomic Physics* (New York: Wiley) appendix J

[6] Oppenheimer J R 1928 *Phys. Rev.* **31** 66

[7] Keldysh L V 1964 *Zh. Eksp. Teor. Fiz.* **47** 1945
Keldysh L V 1965 *Sov. Phys. JETP* **20** 1307